Supporting Information

for

Highly improved the performance of film-based fluorescent sensor via nanomesh scaffold strategy

Quan Liu,*[a] Meng Liu,[a] Dong Li,[a] Kun Li,[a] Haitao Xu,[a] Jiufu Lu,[a] Xianzhao Shao,[a] and Taihong Liu[b]

[a] Shaanxi Province Key Laboratory of Catalytic Foundation and Applications, School of Chemical and Environmental Science, Shaanxi University of Technology, Hanzhong 723001, P. R. China.

[b] Key Laboratory of Applied Surface and Colloid Chemistry of Ministry of Education, School of Chemistry and Chemical Engineering, Shaanxi Normal University, Xi'an 710062, P. R. China.

Table of Contents

1. Synthesis

Molecules **1** and **PBI-Br** (Scheme S1) were synthesized following the previous methods developed Fang's group.[1]

Synthesis of compound *N,N'*-di(2-ethylhexyl)-perylene-3,4,9,10-tetracarboxylic acid diimide (**1**)**:** Under argon atmosphere, 3,4,9,10-perylenetetracarboxylic dianhydride (PTCDA) (6 mmol，2.35 g), *N*-methyl pyrrolidone (25 mL) and 2-ethyl-hexyl amine (13mmol, 1.68 g, 2 mL) was added to the 100 mL round bottom flask. The reaction mixture was refluxed under 110 ^{o}C for 3 h. At the end of the reaction, the reaction liquid was cooled down and filtered, and the filter cake was washed with methanol, acetic acid and anhydrous ether successively. After drying at 50 ^{o}C for 24 h in vacuum, the crude product was obtained. Further separation and purification were carried out through column chromatography on silica gel column ($V_{petroleum\ ether}$: $V_{dichloromethane}$ =1:1), to yield compound **1** as a red solid (87.7%).

^{1}H NMR (600 MHz, $CDCl_3$) *d* (ppm): 8.59 (d, *J*=12 Hz, 4H, Ar-H), 8.49 (d, *J*=12 Hz, 4H, Ar-H), 4.18-4.09 (m, 4H), 1.97-1.95 (m, 2H), 1.42-1.30 (m, 16H), 0.97-0.89 (m, 12H). MS (m/s, MALDI-TOP) calcd for $C_{40}H_{43}N_2O_4$ $[M + H]^+$ 615.32, found 615.37.

Synthesis of compound *N,N'*-di(2-ethylhexyl)-1-bromoperylene-3,4,9,10-tetracarboxylic acid diimide (**PBI-Br**):

Compound **1** (10 mmol, 6.15 g) dissolved in 150 mL CH_2Cl_2 was slowly added to 34 mL Br_2, the reaction mixture was reflux 48 h under 50 ^{o}C. At the end of the reaction, the reaction liquid was cooled down to room temperature. Then pour the reaction solution into a 1000 mL beaker, add 5 g sodium thiosulfate to the mixture system and stir overnight to remove the unreacted bromine in the reaction. The mixture was filtered and washed with ultrapure water for three times. The dark red solid powder was obtained and dried in a vacuum drying oven at 50 ^{o}C for 5 hours. Further separation and purification were carried out through column chromatography on silica gel column ($V_{petroleum\ ether}$: $V_{dichloromethane}$ =1:1), to yield compound **PBI-Br** as a red solid (37.4 %).

^{1}H NMR (600 MHz, $CDCl_3$, ppm) δ: 9.68 (d, *J*=6 Hz, 1H, Ar-H), 8.80 (s, 1H, Ar-H), 8.60-8.58 (m, 3H, Ar-H), 8.47-8.45 (m, 2H, Ar-H), 4.18-4.06 (m, 4H, N-CH_2-), 1.96-1.93 (m, 2H, -CH-), 1.41-1.25 (m, 16H, -CH_2-), 0.96-0.89 (m, 12H, CH_3). ^{13}C NMR (150 MHz, $CDCl_3$) δ (ppm): 163.72, 163.41, 163.31, 162.52, 139.07, 133.69, 133.35, 133.27, 130.94, 130.48, 128.61, 127.99, 127.76,

126.76, 123.66, 123.45, 123.31, 122.98, 122.57, 120.95, 44.44, 37.97, 30.74, 28.71, 24.06, 23.11, 14.13, 10.65. MS (m/s, MALDI-TOP) calcd for $C_{40}H_{42}BrN_2O_4$ $[M + H]^+$ 693.23, found 693.31.

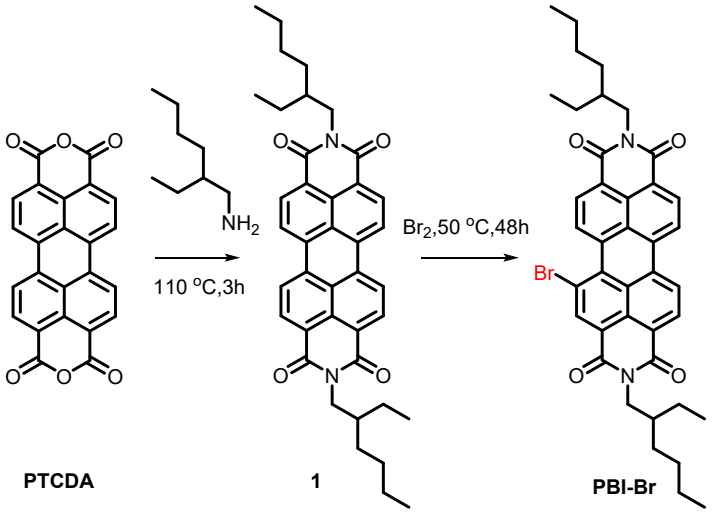

Scheme S1 Molecular structure and synthetic route of compound **PBI-Br**.

2. Characterization

^1H NMR and ^{13}C NMR spectra were acquired on a Bruker AV 600 NMR spectrometer at room temperature using $CDCl_3$ as the solvent and $Si(CH_3)_4$ as the external reference. Matrix-assisted laser desorption/ionization (MALDI) were collected on a Bruker microflex mass spectrometer. Field-emission scanning electron microscopy (FESEM) measurement was performed with a FEI NanoNova 6300 microscope. For sensor testing experiments, 1.0 mL liquid or 1.0 g solid of the typical vapor was sealed in an amber glass bottle (500 mL), and the bottle was kept for 24 h at room temperature (25 °C) for it to reach gas-liquid or gas-solid equilibration. Before measurements, the vapor in the bottle was taken out with a glass syringe and diluted with dry air. For volatile pyridine, it was diluted down to 3750 ppm (1/8 of the saturated vapor) before the sensing test. As for pyridine derivatives, for 2-picoline and diluted down to 1/4 of the saturated vapor (4440 ppm), for 3-picoline (4390 ppm) and 4-picoline (4260 ppm) diluted down to 1/2 of the saturated vapor. Other common solvent vapors use saturated vapor without diluted. Their vapors were used directly without drying. The chamber of the home-made sensing platform was connected to the syringe containing a sample vapor via a plastic pipe and a pump on the other side. In each test, 6 mL of the vapor under concern was pumped into the chamber at a speed of 1.83 mL s^{-1}. The output current of the system was

continuously monitored with analyzer. Each test was repeated at four times, and the time interval between two consequent tests was more than 5 min. All the curves were presented without baseline correction. The environmental (relative) humidity of the surroundings during the tests was around 50%. The actual room temperature was around 25 °C.

3. Specific preparation steps of nanomesh scaffold modified sensor

3.1 Preparation of nanomesh scaffold modified substrate

According to the protocol reported previously[3,4], the monolayer of the polystyrene (PS) spheres on the glass substrate were fabricated. Briefly, the PS spheres were dispersed to form a monolayer at the air/ water interface. The monolayer of the spheres was then transferred onto a pre-cleaned glass substrate. The nanomesh scaffold modified glass substrate were prepared by dispersing 200 μL silica sol (34 wt. % suspension in H_2O) onto the glass substrate modified with a monolayer of the PS spheres via spin-coating method. Glue at 500 rpm for 30 s, and then spin at 2000 rpm for 1 min. After being dried at room temperature, the substrate was immersed in toluene to remove the PS particles.

Different concentrations of silica sol can be used to regulate the depth of bowl cavity. Silica sol with concentrations of 3%, 5%, 7%, 10% and 15% were selected respectively. The hole depth of nanomesh scaffold modified substrate was characterized by SEM and AFM. It can be clearly seen from the SEM image that when the silica sol concentration is 3% ~ 5% (Fig. S1a), the silica sol in the gap is evenly filled and the micro cavity size is uniform, which is suitable for the silica sol concentration; When the silica sol concentration increases to 7% ~ 10% (Fig. S1b), the silica sol in the gap is filled too much, so that part of the microcavity is covered by silica sol, which is not suitable for the filling concentration of silica sol; When the silica sol concentration is further increased to 15%, an interesting phenomenon is observed. The template also has a relatively uniform silica sol filling, but different from the filling at 3% ~ 5%, the silica sol filling height is low. It is considered that this is the result of peeling together due to the large concentration of silica sol covering the surface of PS microspheres. In order to verify the experimental results, AFM analysis was carried out on the templates with 3% and 15% silica sol concentration respectively (Fig. S2).

The micropore height of the template with 3% silica sol concentration is about 300nm, while the

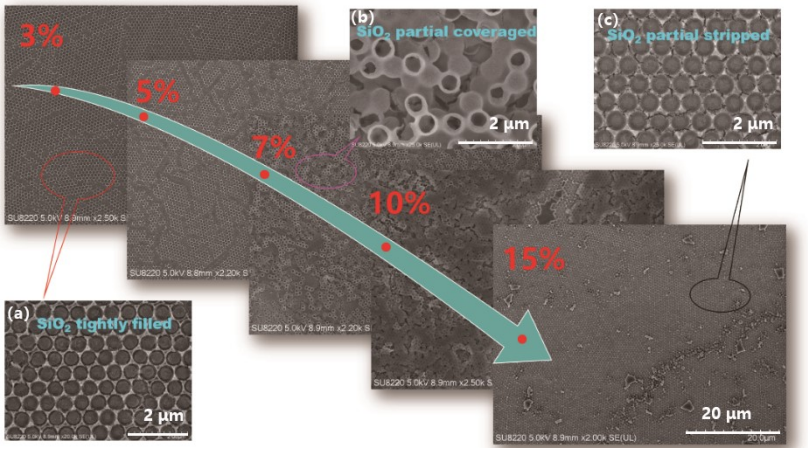

micropore height of the template with 15% silica sol concentration is about 200nm.

Fig. S1 SEM images of nanomesh scaffold modified substrate (a) the concentration of silica sol is 3%; (b) the concentration of silica sol is 7%; (c) the concentration of silica sol is 15%. (scale bar = 2 μm)

Fig. S2 AFM images of nanomesh scaffold modified substrate (a) the concentration of silica sol is 3% and (b) the concentration of silica sol is 15%; Cross-section profiles of AFM topographic images of (c) the concentration of silica sol is 3% and (d) the concentration of silica sol is 15%, of which x-axis represents the length of the cross-section profiles and y-axis represents the roughness of the cross-section profiles.

3.2 Preparation of PBI-Br nanofibers

PBI-Br nanofibers were fabricated by injecting 0.5 mL chloroform solution of PBI-Br molecules (0.15 mM) into 3 mL ethanol in a test tube followed by aging 5 h. The nanofibers thus formed can be transferred onto the surface of nanomesh scaffold modified substrate by pipetting.

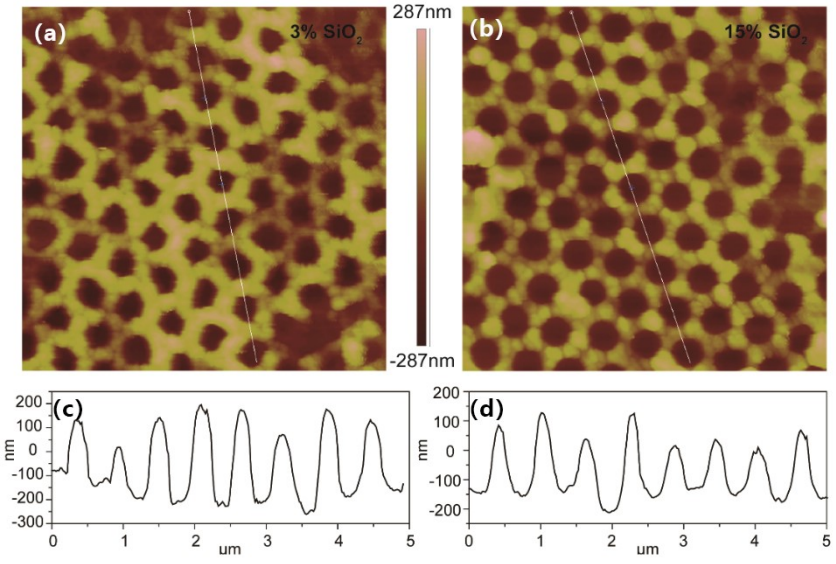

4. NMR spectra data

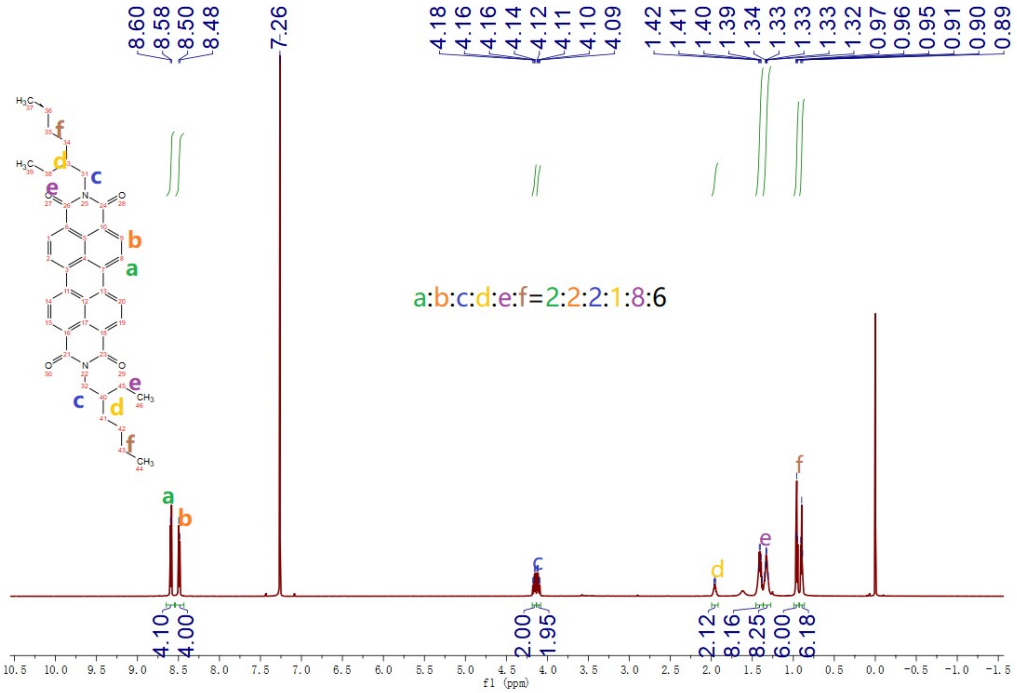

Fig. S3 ^{1}H NMR spectrum of **1**.

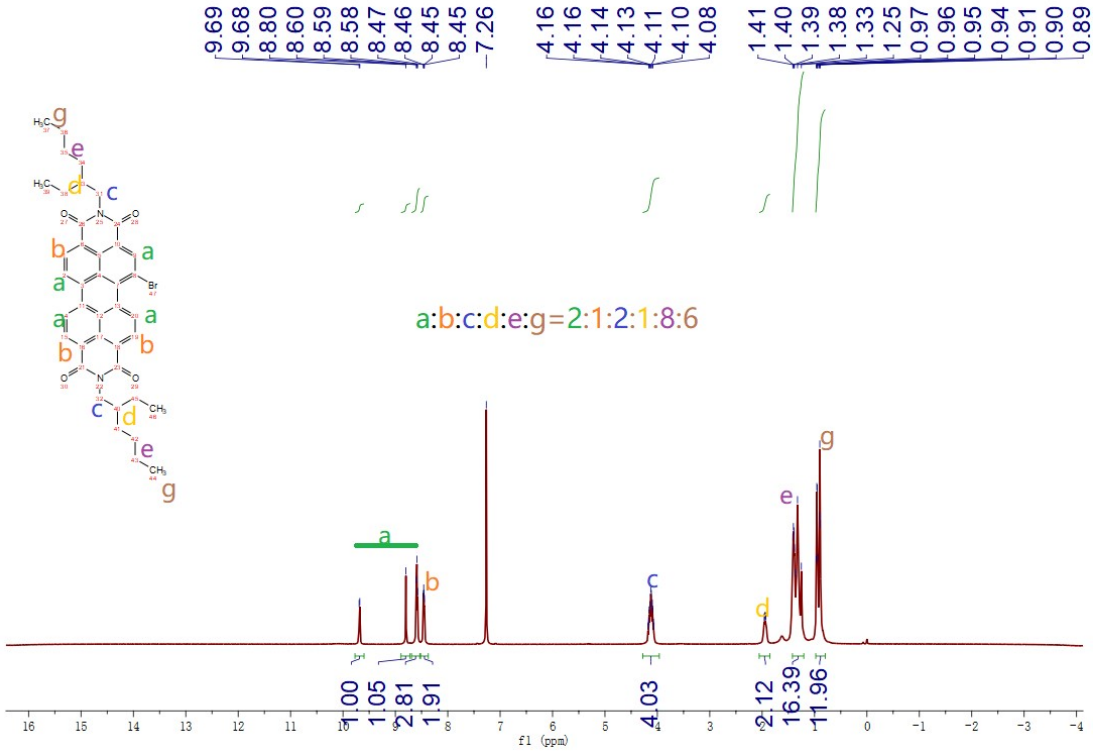

Fig. S4 ^{1}H NMR spectrum of **PBI-Br**.

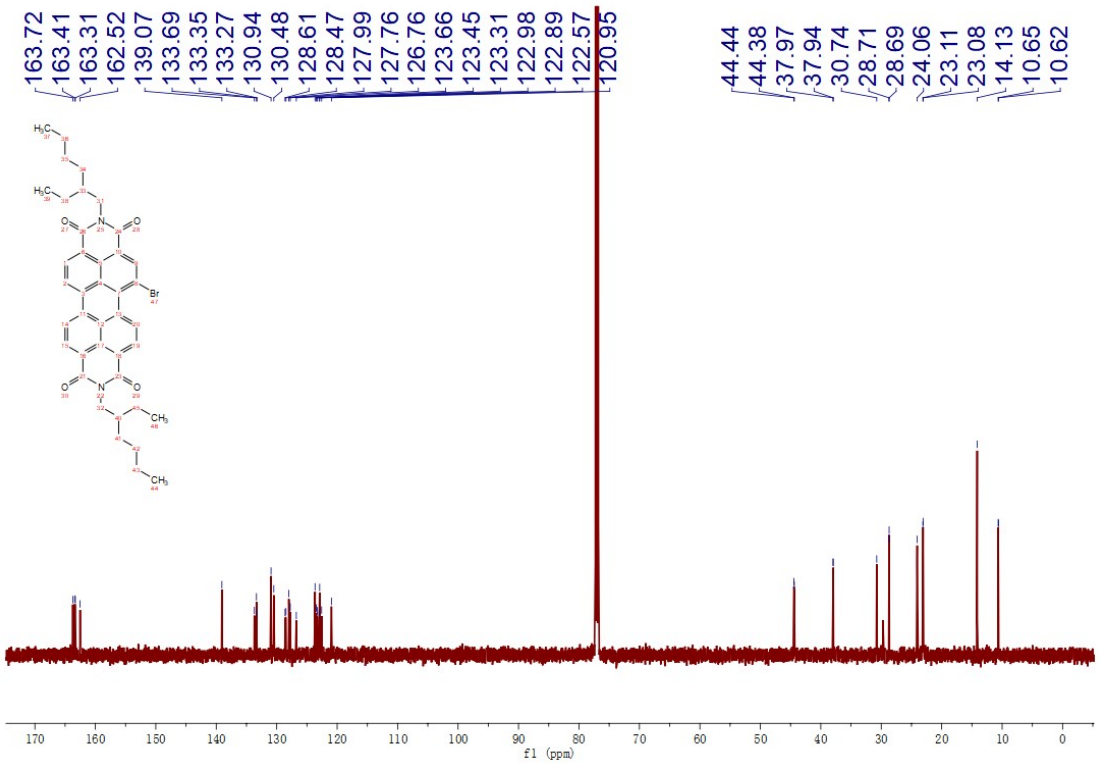

Fig. S5 ^{13}C NMR spectrum of **PBI-Br**.

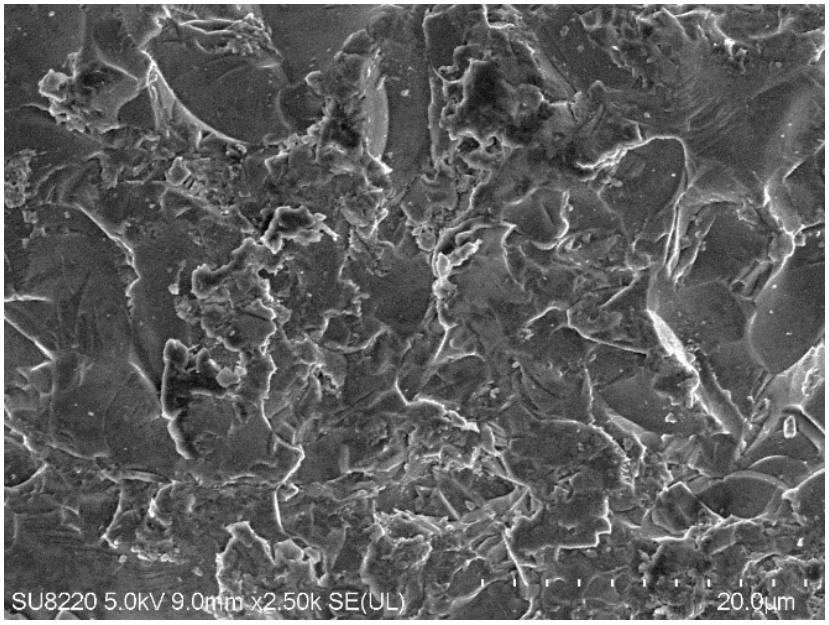

Fig. S6 SEM image of the ground glass substrate (scale bar = 20 μm).

5. Sensing performance of sensor

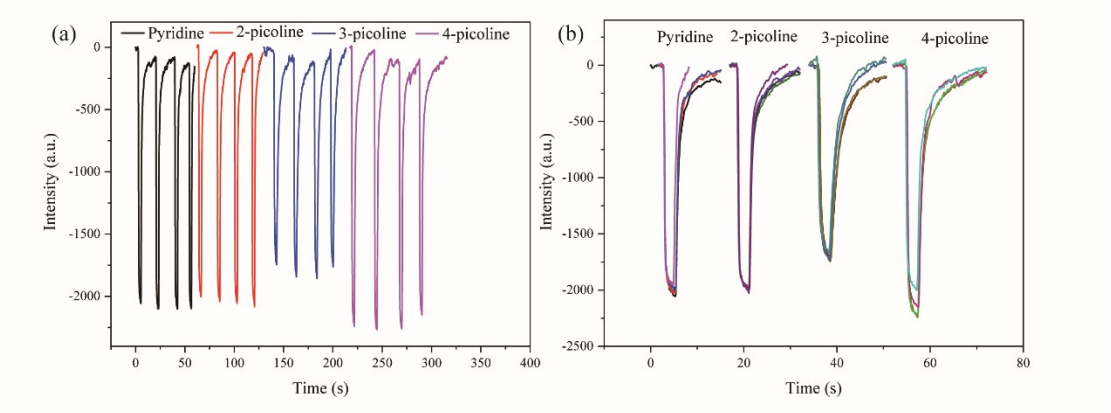

Fig. S7 (a) Response intensity of the nanomesh scaffold modified sensor (the hole depths of substrate is 300 nm) recorded with different pyridine derivatives (c_{pyridine} =3750 ppm, $c_{\text{2-picoline}}$ = 4440 ppm, $c_{\text{3-picoline}}$ = 4390 ppm, and $c_{\text{4-picoline}}$ = 4260 ppm); (b) Graph of four sensing signal superposition.

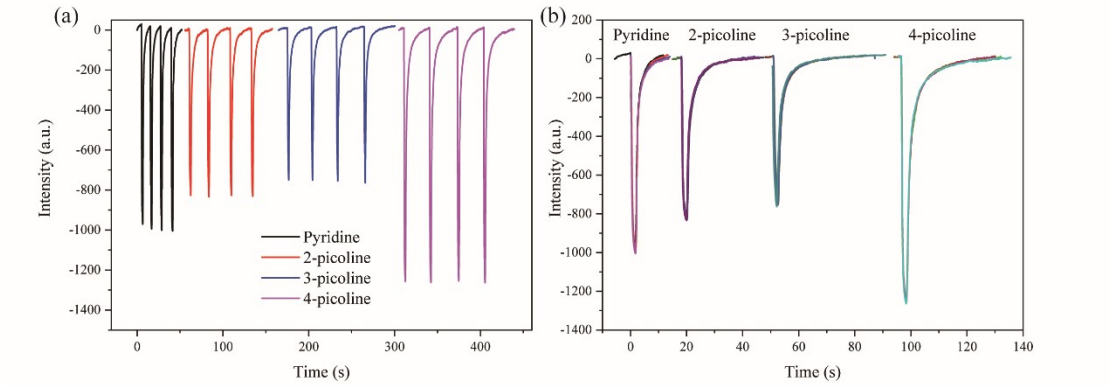

Fig. S8 (a) The intensity of the ground glass-based sensor recorded with different pyridine derivatives (c_{pyridine} =3750 ppm, $c_{\text{2-picoline}}$ = 4440 ppm, $c_{\text{3-picoline}}$ = 4390 ppm**,** and $c_{\text{4-picoline}}$ = 4260 ppm**)**; (b) Graph of four sensing signal superposition.

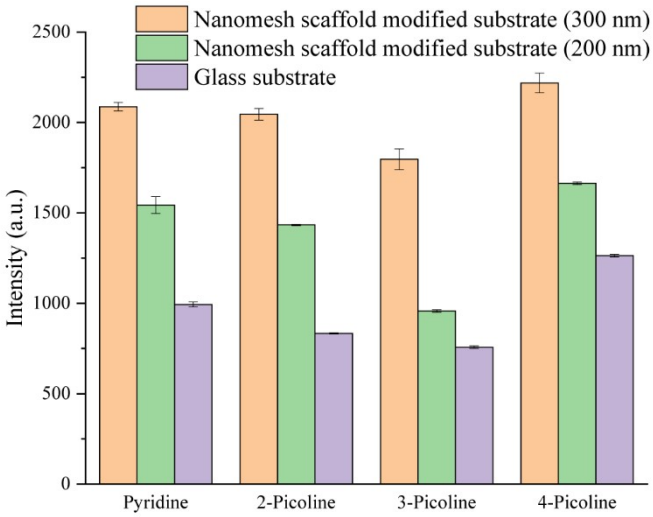

Fig. S9 Comparison diagram of response intensity of sensor based on the hole depth of the nanomesh scaffold modified substrate is 300 nm (yellow), 200nm (green) and glass substrate (purple) to different pyridine derivatives. (c_{pyridine} =3750 ppm, $c_{\text{2-picoline}}$ = 4440 ppm, $c_{\text{3-picoline}}$ = 4390 ppm, and $c_{\text{4-picoline}}$ = 4260 ppm)

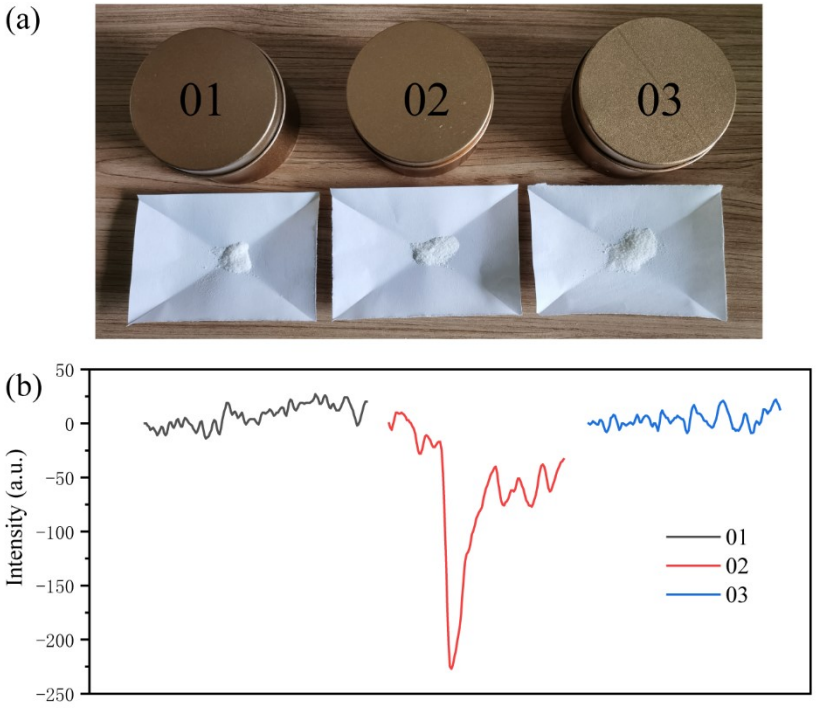

Fig. S10 (a) Simulated field tests for evaluating the performance of the nanomesh scaffold modified sensor. Three boxes with sugar power (01), 2, 6-dicarboxyridine (02), and salt power (03); (b) response intensity of the nanomesh scaffold modified sensor to the three boxes.

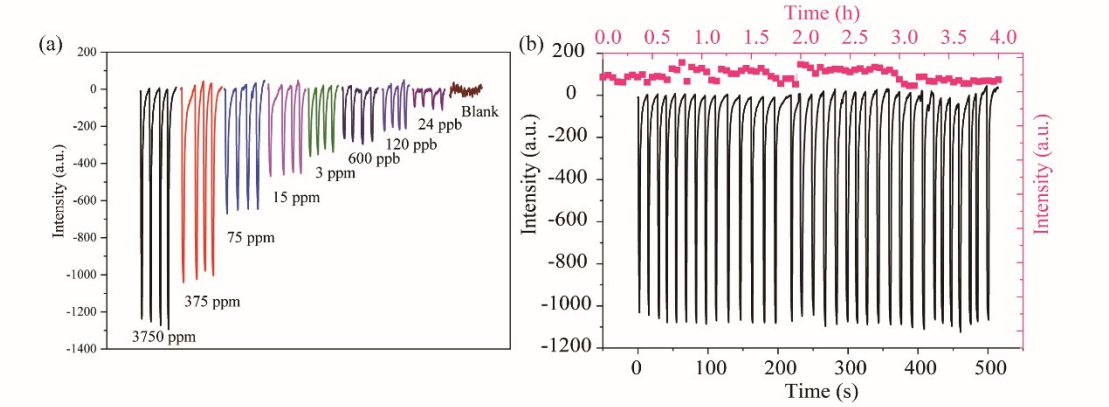

Fig. S11 (a) Signal intensity of the ground glass-based sensor recorded at different pyridine concentrations (varying from 24 ppb to 3750 ppm, 25 °C); (b) Reusability and photochemical stability test of the ground glass based sensor towards pyridine vapor (c = 3750 ppm, 25 °C).

Table S1 Performance comparison of present pyridine sensor with the reported works.

NO.[Ref.]	Sensors method	Analyte(s)	Gas/ Aqueous	LOD	T_{res}
1	Fluorescence (This work)	Pyridine, PDA	Gas	4.8 ppb for Pyridine	＜1 s
2[4]	HPLC	Pyridine	Gas	-	-
3[5]	GC-MS	Pyridine	Gas	-	-
4[6]	HRGC-MS	Pyridine	Gas	-	-
5[7]	RP-HPLC–ESI-MS/MS	Pyridine	Gas	1.74 - 14.32 ng/cig	-
6[8]	Chemiresistive	Pyridine and its derivatives	Gas	375 ppb for Pyridine	＜1 s
7[9]	Visual Sensing	Pyridine	Aqueous	1.0 mmol·dm^{-3} - 5.0 mol·dm^{-3}	15 mins
8[10]	SERS	Pyridine derivatives	Aqueous	3·10^{-5} mol·dm^{-3}	10 mins
9[11]	Fluorescence	Pyridine	Aqueous	6.76 ×10 $^{-5}$ M	-
10[12]	Fluorescence	PDA	Aqueous	0 - 7.0 μM	-
11[13]	Chemical Sensing	Pyridine Benzylamine	Aqueous	5.7 μg L^{-1}	-
12[14]	Chemometrics assisted spectrophotometric	Pyridine	Aqueous	0.67-51.7 μg mL^{-1}	-

References

[1] G. Wang, C. Shang, L. Wang, H. Peng, S. Yin, Y. Fang, Can the excited state energy of a

pyrenyl unit be directly transferred to a perylene bisimide moiety? *J. Phys. Chem. B,* **2016**, 120, 11961-11969.

[2] S. Tian, Q. Zhou, Z. Gu, X. Gu, J. Zheng, Fabrication of a bowl-shaped silver cavity substrate for SERS-based immunoassay. *Analyst*, **2013**, 138, 2604-2612.

[3] S. Tian, Q. Zhou, Z. Gu, X. Gu, L. Zhao, Y. Li, J. Zheng, Hydrogen peroxide biosensor based on microperoxidase-11 immobilized in a silica cavity array electrode. *Talanta*, **2013**, 107, 324–331.

[4] R. W. Frei, K. Beall, R. M. Cassidy, Determination of aromatic nitrogen heterocycles in air samples by high-speed liquid chromatography. *Microchim. Acta.*, **1974**, *5*, 859–869.

[5] D. J. Eatough, C. L. Benner, J. M. Bayona, G. Richards, J.D. Lamb, M. L. Lee, Chemical composition of environmental tobacco smoke. 1. Gas-phase acids and bases. *Environ. Sci. Technol.*, **1989**, *23*, 679–687.

[6] C. W. Bayer, M. S. Black. Capillary chromatographic analysis of volatile organic compounds in the indoor environment. *J. Chromatogr. Sci.*, **1987**, *25*, 60–64.

[7] S. Saha, R. Mistri, B. C. Ray. Determination of pyridine, 2-picoline, 4-picoline and quinoline from mainstream cigarette smoke by solid-phase extraction liquid chromatography/electrospray ionization tandem mass spectrometry. *J. Chromatogr. A*, **2010**, *1217*, 307–311.

[8] Q. Liu, C. Zhao, X. Shao, W. Wang, X. Ji, High sensitive pyridine chemiresistive sensors based on azacyclobutane modified perylene bisimide derivatives. *Dyes Pigm.*, **2021**, *185*, 108902.

[9] B. Lv, C. Cheng, Y. Mo, H. Yuan, D. Xiao. A simple strategy for pyridine visual sensing by the in-situ formation of tetranuclear copper iodine pyridine microcrystalline film on copper foil. *Thin Solid Films*, **2008**, *516*, 7812–7815.

[10] E. Proniewicz, B. Gralec, T. K. Olszewski, B. Boduszek. Aqueous platinum nanoparticles solution for the detection of pyridine derivatives of aminophosphinic acid. Influence of positional isomerism. *Appl. Surf. Sci.*, **2017**, *425*, 941–947.

[11] Z. Li, J. Ma, Y. Zong, Y. Men. ZnS nanoparticles for high-sensitive fluorescent detection of pyridine compounds. *J. Alloys Compd.*, **2013**, *559*, 39–44.

[12] K. Luan, R. Meng, C. Shan, J. Cao, J. Jia, W. Liu, Y. Tang. Terbium functionalized micelle nanoprobe for ratiometric fluorescence detection of anthrax spore biomarker. *Anal. Chem.*, **2018**, *90*, 3600–3607.

[13] G. G. Huang, C. J. Lee, J. Yang, C. H. Chang, M. Sathiyendiran, Z. Z. Lu, Rheniumbased molecular trap as an evanescent wave infrared chemical sensing medium for the selective determination of amines in air. *ACS Appl. Mater. Interfaces*, **2016**, *8*, 35634−35640

[14] K. P, Singh, N. Basant, A. Malik, V. K. Singh, D. Mohan. Chemometrics assisted spectrophotometric determination of pyridine in water and wastewater. *Anal. Chim. Acta.*, **2008**, *630*, 10–18.